6-2023

Exceptional point based lattice gyroscopes

Masoumeh Izadparast

Gururaj V. Naik

Henry O. Everitt

Hamidreza Ramezani

Research Article | Vol. 13, No. 6 / 1 Jun 2023 / Optical Materials Express 1547
Optical Materials EXPRESS

Exceptional point based lattice gyroscopes

MASOUMEH IZADPARAST,[1] GURURAJ V. NAIK,[2] HENRY O. EVERITT,[2,3] AND HAMIDREZA RAMEZANI[1,*]

[1]Department of Physics and Astronomy, University of Texas Rio Grande Valley, Edinburg, Texas 78539, USA
[2]Department of Electrical and Computer Engineering, Rice University, Houston, Texas 77005, USA
[3]U.S. Army DEVCOM Army Research Laboratory-South, Houston, Texas 77005, USA
*hamidreza.ramezani@utrgv.edu

Abstract: Ring laser gyroscopes (RLGs) based on non-Hermitian exceptional points (EPs) have garnered much recent interest due to their exceptional sensitivity. Such gyroscopes typically consist of two-ring laser resonators, one with loss and one with an equal amount of optical gain. The coupling strength between these ring resonators is a key parameter determining the sensitivity of EP-based RLGs. Here we explore how the exceptional sensitivity demonstrated in this coupled dimer may be further enhanced by adding more dimers in an array. Specifically, we propose two types of ring laser gyroscope lattice arrays, each composed of N coupled dimers arrayed serially or concentrically with periodic boundary conditions, that guide counter-propagating photons in a rotating frame. Using coupled mode theory, we show that these lattice gyroscopes exhibit an enhanced effective coupling rate between the gain and loss resonators at the EP, thereby producing greater sensitivity to the angular rotation rate than their constituent dimers. This work paves the way toward EP-based RLGs with the necessary sensitivity for GPS-free navigation.

1. Introduction

Ring laser gyroscopes (RLGs) use the Sagnac effect to measure rotation rates in inertial navigation systems. When two counter-propagating light rays with the same frequency pass through a ring resonator in a rotational reference frame, they acquire opposite frequency shifts. These frequency shifts $\Delta\omega_s$ are linearly related to the rotation rate Ω of the single ring resonator through

$$\Delta\omega_s = \frac{4\pi R\Omega}{\lambda}, \tag{1}$$

where R is the radius of the ring, and λ is the wavelength of light [1]. Thus, by monitoring the Sagnac frequency splitting, the gyration rates in navigational systems may be measured. Unfortunately, measuring this splitting becomes challenging for even moderate rotation speeds ($\lesssim 10^\circ$ per second). Greater sensitivity is needed for slower rotation rates, so alternatives are needed for precision inertial navigation [2].

Many techniques have been studied for enhancing the sensitivity of RLGs. [1,3–11] Among them, perhaps the most promising are those based on exceptional point (EPs) in non-Hermitian systems [11–21]. Non-Hermitian systems are open systems that exhibit physical features of tremendous interest [22–30], especially for sensing using coupled gain-loss resonators because the phase transition that occurs at an EP makes them extremely sensitive to perturbations. Thus, the addition of non-Hermitian potentials to an RLG allows them to operate near an EP singularity and significantly enhances their sensitivity. The Hilbert space of such systems becomes distorted at the EP, producing a degeneracy-induced intersection of complex Riemann sheets associated with the spectrum of the system. For an $\mathcal{M}^{\text{th}}$ order EP, with an integer $\mathcal{M}$ being two or larger, the spectrum around this intersection and the sensitivity of the system is given by the $\mathcal{M}^{\text{th}}$-root of the coupling strength between the gain and loss resonators, independent of the radius of the rings. [14] Thus, any small perturbation around the EP will amplify by its $\mathcal{M}^{\text{th}}$ root. This effect

#483155 https://doi.org/10.1364/OME.483155
Journal © 2023 Received 12 Dec 2022; revised 7 Apr 2023; accepted 13 Apr 2023; published 8 May 2023

Optical Materials EXPRESS

has been discussed in detail in Ref. [11] where the EP-based gyroscopes using various methods are thoroughly reviewed.

A recent experimental demonstration of a non-Hermitian RLG operated near a second-order EP used a Helium-Neon gain medium in a triangular cavity [14]. The clockwise (CW) and counter-clockwise (CCW) modes were modified to establish non-Hermiticity by inducing a differential loss in the system, mimicking gain-loss non-Hermitian RLGs. Because it was a second-order EP, the frequency shift was proportional to the square root of Sagnac frequency, so a very small rotation of the system produced a large frequency splitting and enhanced its ability to measure very low rotation rates by many orders of magnitude. A more recent prototype has demonstrated the ability to measure the 0.004° per second rotation speed of the earth, a needed capability for GPS-free navigation [2].

There are limits to how much sensitivity enhancement is possible with this approach. The sensitivity of EP-based RLGs is determined by the coupling strength between the loss and gain ring resonators. This coupling strength cannot be arbitrarily increased for very practical reasons: decreasing the gap between the two ring resonators increases the coupling strength, but the smallest achievable gap distance is limited by the fabrication process. Alternative routes to engineer the effective coupling between the two rings of an EP-based RLG are needed.

Here we propose an alternative based on loss-gain ring dimers in an array with periodic boundary conditions. We consider two geometries here, one arrayed in a serial manner and one arrayed in a concentric geometry, each of which generates an effective coupling between the modes propagating in the lattice composed of loss and gain rings. This ultimately creates rotation rate sensitivity greater than that of a single dimer.

2. Serial ring lattice

Consider N dimers composed of identical rings with resonance frequency ω_0 whose gain (γ_G<0) and loss (γ_L>0) are balanced. Without loss of generality, we assume $\omega_0 = 0$. The rings are coupled serially so as to form a periodic boundary condition in which each ring is also coupled to its nearest neighbor ring. The counter-propagating light rays travel within the coupled rings of the lattice in a manner characterized by the intra- and inter-dimer coupling constants κ and ν, respectively. We assume that these coupling constants are real and that $\kappa = m\nu$, for which $0 \leq m \in \Re$. In order to illustrate the potential benefit of lattice geometries, we do not include noise in our calculations and postpone the study of noise to future research. Fig. (1-a) schematically illustrates an example of such a lattice with $N = 6$ dimers, whose frame is rotating clockwise with the angular rotation rate Ω.

Using coupled-mode theory [31], we can write a set of Schrödinger-like equations indicating the diffraction dynamics of the electric field amplitudes within the gain (ψ_n) and loss (ϕ_n) rings of the n^{th} dimer, as

$$\begin{aligned} \left(i\frac{d}{dt} - i\gamma_G + \Delta\omega_s\right)\psi_n + \kappa\phi_n + \nu\phi_{n-1} = 0, \\ \left(i\frac{d}{dt} - i\gamma_L - \Delta\omega_s\right)\phi_n + \kappa\psi_n + \nu\psi_{n+1} = 0, \end{aligned} \tag{2}$$

where t is time, and $\Delta\omega_s$ is the shift in the resonant frequency of the rings due to the Sagnac effect of Eq. (1).

To analyze the setup further, it is instructive to use the momentum representation of the field amplitudes. For the $\psi_n(t)$ component this would be given by

$$\psi_n(t) = \frac{1}{2\pi}\int_{-\pi}^{\pi} dq\bar{\psi}_q(t)\, e^{inq}, \tag{3}$$

in which $\bar{\psi}_q(t)$ corresponds to the field amplitude in momentum space, q with is the wavenumber and the interval of the integral covers the Brillouin zone $-\pi \leq q \leq \pi$. A similar equation can be

Optical Materials EXPRESS

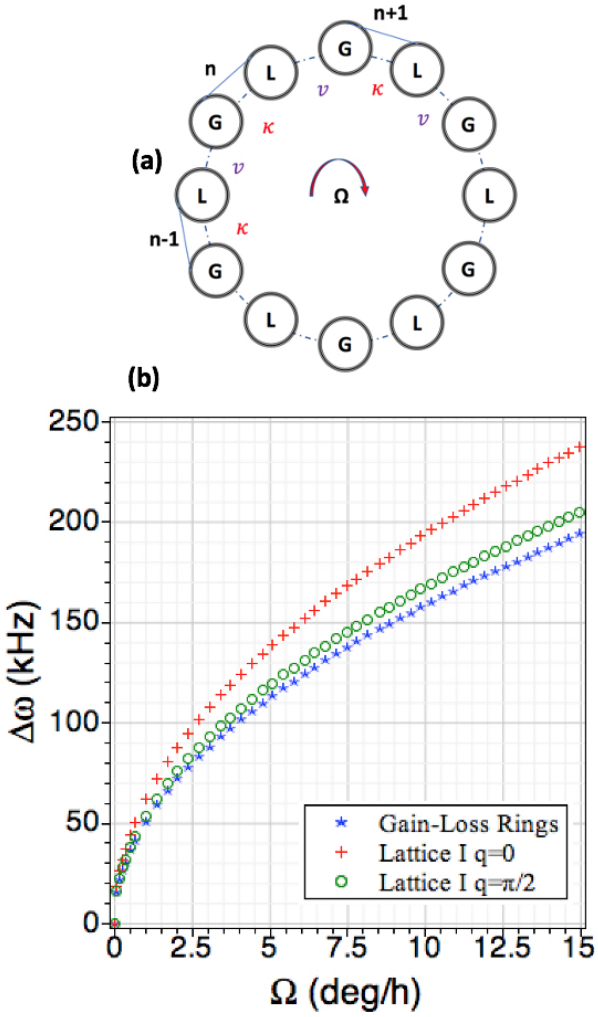

Fig. 1. (a) Schematic diagram of a serial ring lattice comprised of $N = 6$ coupled gain (G) and loss (L) rings, with coupling constants $\kappa = 10^{12}\ s^{-1}$ and $\nu = 0.5\kappa\ s^{-1}$. In this model the CW mode in one resonator couples to a CCW mode of the nearest neighbor resonator. The CW and CCW modes experience the Sagnac effect with opposite signs. (b) The beat frequency $\Delta\omega$ for wavenumbers $q = 0$ (+) and $\frac{\pi}{2}$ (◯) as a function of rotation rate Ω, compared to the single dimer case (⋆).

Optical Materials EXPRESS

written for ϕ_n. Notice that for a lattice with a periodic boundary condition, the wavenumbers become quantized as $q = \frac{2\pi m}{N}$ with $m = 0, 1, \ldots, N$.

Substituting Eq. (3) and the similar equation for ϕ_n into (2), we obtain a 2×2 Hamiltonian for the coupled cavities

$$H = \begin{pmatrix} -i\gamma_G + \Delta\omega_s & \kappa + \nu e^{-iq} \\ \kappa + \nu e^{iq} & -i\gamma_L - \Delta\omega_s \end{pmatrix}. \tag{4}$$

Applying stationary solutions to this Hamiltonian determines the band structure $\omega_\pm(q)$ of the system

$$\begin{aligned} \omega_\pm = & -i\frac{(\gamma_G + \gamma_L)}{2} \\ & \pm \sqrt{\kappa^2 + 2\kappa\nu\cos q + \nu^2 - \left(i\Delta\omega_s + \frac{\gamma_G - \gamma_L}{2}\right)^2}. \end{aligned} \tag{5}$$

For the non-rotating case where $\Delta\omega_s = 0$, we find from Eq. (5) that when

$$\gamma_G - \gamma_L = 2\sqrt{\kappa^2 + \nu^2 + 2\kappa\nu\cos q}, \tag{6}$$

the system is at its exceptional point for the mode associated with the corresponding q, the eigenvectors of the Hamiltonian (4) abruptly coalesce, and the system lases at a single frequency.

However, when the system starts rotating with $\Delta\omega_s$ the system departs from exceptional point and two supermodes will be created with a beat frequency $\Delta\omega$ [14,16]. In other words, by operating at the exceptional point, the beat frequency between the two branches of the band structure ($\Delta\omega = \omega_+ - \omega_-$) will be given by

$$\Delta\omega = 2\sqrt{\Delta\omega_s^2 - 2i\Delta\omega_s\left(\sqrt{\kappa^2 + \nu^2 + 2\kappa\nu\cos q}\right)}. \tag{7}$$

Note first that the dispersion relation Eq. (5) and beat frequency Eq. (7) of the serial lattice model is invariant under the exchange of κ and ν. Thus, the beat frequency remains the same if we exchange intra- and inter-dimer coupling strengths. Second, the beat frequency is a function of the wavenumber q, so one can tune the beat frequency by varying the wavenumber. Beyond RLGs, this might be useful for other applications, such as tunable optomechanical modulators and filters.

Furthermore, it is clear from Eq. (7) that the largest beat frequency $|\Re(\omega_+ - \omega_-)|$ occurs at $q = 0$ where

$$\Delta\omega = 2\sqrt{\Delta\omega_s^2 - 2i\Delta\omega_s(\kappa + \nu)}. \tag{8}$$

Because the effective coupling is the sum of the intra- and inter-dimer couplings in the system, we can increase the beat frequency by increasing either. This is the advantage over a system with only a single dimer composed of two coupled ring resonators, whose beat frequency $\Delta\omega = 2\sqrt{\Delta\omega_s^2 - 2i\kappa\Delta\omega_s}$ only contains the intra-dimer coupling term.

To illustrate this advantage, Fig. (1-b) compares the beat frequency of an $N = 6$ serial ring lattice to the single dimer model in Ref. [14], as a function of Ω for $q = 0$ and $\frac{\pi}{2}$. We use the experimentally reported parameters $R = 100\ \mu m$, $\lambda = 1.55\ \mu m$, $\kappa = 10^{12}\ s^{-1}$ [14], and assume an inter-dimer coupling constant $\nu = 0.5\kappa\ s^{-1}$. We see that because of the $\cos q$ term the lattice model provides a higher beat frequency and greater sensitivity for $0 \le q \le \pi/2$ than in the single dimer case reported in Ref. [14], while for $q > \pi/2$ the lattice becomes less sensitive. Note that the mode associated with $q = 0$ is the last mode that enters the broken phase or weak-coupling regime; all other modes are already in the broken phase with imaginary energy eigenvalues. Consequently, to operate at $q = 0$ the gain profile must be tuned such that other modes do not lase, even if they are in the broken phase.

Optical Materials EXPRESS

3. Concentric ring lattice

In this section, we introduce an alternative lattice to show the power of our method for modifying the effective coupling and achieving higher sensitivity. The second model is again composed of a lattice of dimers, characterized by intra-dimer coupling constant κ, with a periodic boundary condition, as depicted in Fig. (2-a). The difference from the serial lattice is in the way the inter-dimer couplings ν occur: each dimer ring in the concentric lattice is coupled to two rings in adjacent dimers, not just one as in the serial case (compare Figs. 1(a) and 2(a)).

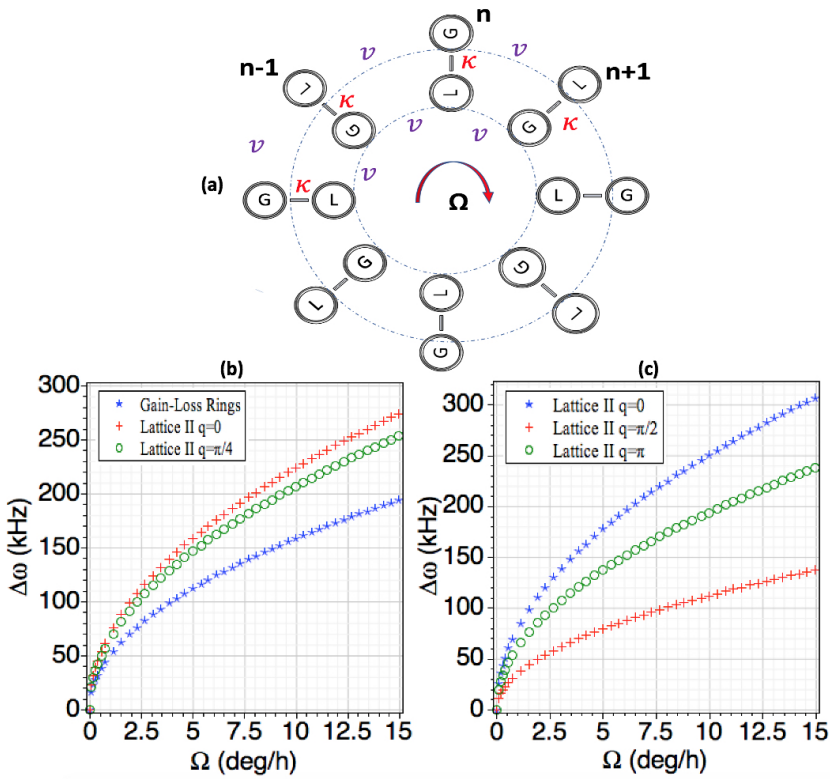

Fig. 2. (a) The concentric lattice model with $N = 8$ dimers aligned radially along the circumference of a circle. The rings interact internally with κ and are coupled to the rings of the adjacent dimers through coupling constant ν. The frame is rotating clockwise with the angular speed of Ω, while the light rays propagate through the gain-loss cavities in opposite directions. (b) Beat frequencies for $\kappa > \nu$ and wavenumbers $q = 0$ (+) and $\frac{\pi}{4}$ (◯), compared to the single dimer case (★). (c) Beat frequencies for $\nu > \kappa$ for three different wavenumbers.

Following the same coupled mode theory formalism we developed for the serial lattice, we calculate the wave function and the diffraction dynamics of the electric field amplitudes in the concentric lattice. In this case, we find that the amplitudes of the electric fields within the gain and loss rings of the n^{th} dimer are given by

$$\begin{aligned}\left(i\frac{d}{dt} - i\gamma_G + \Delta\omega_s\right)\psi_n + \kappa\phi_n + \nu\left(\phi_{n-1} + \phi_{n+1}\right) = 0,\\ \left(i\frac{d}{dt} - i\gamma_L - \Delta\omega_s\right)\phi_n + \kappa\psi_n + \nu\left(\psi_{n-1} + \psi_{n+1}\right) = 0.\end{aligned} \tag{9}$$

Optical Materials EXPRESS

The Hamiltonian of Eq. (9) in momentum space is then given by

$$H = \begin{pmatrix} -i\gamma_G + \Delta\omega_s & \kappa + 2\nu\cos q \\ \kappa + 2\nu\cos q & -i\gamma_L - \Delta\omega_s \end{pmatrix}. \tag{10}$$

From this, we can calculate the beat frequency from the band structure eigenfrequencies as

$$\Delta\omega = 2\sqrt{(\kappa + 2\nu\cos q)^2 - \left(i\Delta\omega_s + \frac{\gamma_G - \gamma_L}{2}\right)^2}, \tag{11}$$

for which the $\Delta\omega_s = 0$ degeneracy occurs when

$$\gamma_G - \gamma_L = 2\,(\kappa + 2\nu\cos q)\,. \tag{12}$$

To operate at the exceptional point and obtain the highest sensitivity of the concentric lattice, we apply Eq. (12) into (11) and find a new relationship for the beat frequency, namely

$$\Delta\omega = 2\sqrt{\Delta\omega_s^2 - 2i\Delta\omega_s\,(\kappa + 2\nu\cos q)}. \tag{13}$$

In comparison with Eq. (7), notice that the beat frequency here is not invariant under the exchange of the two coupling values. Thus, exchanging the couplings will change the sensitivity of the gyroscope, as shown in Fig. (2-b,c).

Figure (2-b) plots the beat frequency of an $N = 8$ concentric ring lattice with respect to Ω for $\kappa = 10^{12}\ s^{-1}$ and $\nu<\kappa$ for wavenumbers $q = 0$ and $\frac{\pi}{4}$. Notice the enhanced sensitivity over the simple gain-loss RLG dimer, especially for $q = 0$, when intra-dimer coupling dominates inter-dimer coupling. Alternatively, Fig. (2-c) plots the latter relation for $\nu = 10^{12}\ s^{-1}$ for $\nu>\kappa$ for three different values of wavenumber q. It is clear that sensitivity strongly depends on q. The mode that enters the broken regime first has less sensitivity than the one that enters last. As before, the system must be operated such that the modes already in the broken regime do not gain enough to start lasing.

Before closing this section we would like to mention that in order to create the concentric ring configuration, one might need to put the outer rings out of plane such that they become parallel to the rings in the inner circle.

4. Conclusion

In summary, we introduced two lattice geometries of coupled gain-loss resonator dimers for enhancing sensitivity over single dimer EP-based RLGs. The coupled gain-loss ring dimer in a lattice with periodic boundary conditions enhanced effective coupling between the ring dimers. We studied two lattice configurations, a serial ring lattice, and a concentric ring lattice, using coupled mode theory. We showed that for any mode with $q \neq \pi$ the effective coupling strength between the two modes of the lattice can be greater than the coupling strengths between any two adjacent rings. Hence, the sensitivity of RLGs based on these configurations would also be higher than that of single dimers. Although both configurations proposed in this letter are working based on second-order exceptional points, the second one breaks the symmetry in the effective couplings between the modes and allows for better control of the system. However, this comes with a price of a mode difficult fabrication process. The two configurations considered here may be generalized to other configurations with the same rotational symmetry. Lattices of coupled dimers may pave the way for integrated EP-based RLGs with the extreme sensitivity required for measuring tiny rotation rates. However, excessive noise at EPs might still limit their use [32–36]. Nonlinear effects could suppress excessive noise near EPs [28]. Together with such noise-suppression techniques, lattices of coupled dimers are promising for integrated EP-based RLGs with a sensitivity high enough to measure earth rotation and enable GPS-free navigation.

Optical Materials EXPRESS

Funding. National Science Foundation (PHY-2012172, OMA-2231387, ECCS-1935446); Army Research Office (W911NF2010276, W911NF2120031).

Acknowledgments. The views and conclusions contained in this document are those of the authors and should not be interpreted as representing the official policies, either expressed or implied, of the Army Research Office or the U.S. Government. The U.S. Government is authorized to reproduce and distribute reprints for Government purposes notwithstanding any copyright notation herein.

Disclosures. The authors declare no conflicts of interest related to this article.

Data Availability. The data that support the findings of this study are available from the corresponding author upon reasonable request.

References

1. W. W. Chow, J. Gea-Banacloche, L. M. Pedrotti, V. E. Sanders, W. Schleich, and M. O. Scully, "The ring laser gyro," Rev. Mod. Phys. **57**(1), 61–104 (1985).
2. Y.-H. Lai, M.-G. Suh, Y.-K. Lu, B. Shen, Q.-F. Yang, H. Wang, J. Li, S. H. Lee, K. Y. Yang, and K. Vahala, "Earth rotation measured by a chip-scale ring laser gyroscope," Nat. Photonics **14**(6), 345–349 (2020).
3. M. Faucheux, D. Fayoux, and J. J. Roland, "The ring laser gyro," J. Opt. **19**(3), 101–115 (1988).
4. A. Lawrence, "The ring laser gyro," in *Mechanical Engineering Series*, (Springer New York, 1998), pp. 208–224.
5. B. Z. Steinberg, "Rotating photonic crystals: A medium for compact optical gyroscopes," Phys. Rev. E **71**(5), 056621 (2005).
6. M. N. Armenise, C. Ciminelli, F. Dell'Olio, and V. M. N. Passaro, *Advances in Gyroscope Technologies* (Springer Berlin Heidelberg, 2011).
7. H. Lee, T. Chen, J. Li, K. Y. Yang, S. Jeon, O. Painter, and K. J. Vahala, "Chemically etched ultrahigh-q wedge-resonator on a silicon chip," Nat. Photonics **6**(6), 369–373 (2012).
8. J. Zhang, H. Ma, H. Li, and Z. Jin, "Single-polarization fiber-pigtailed high-finesse silica waveguide ring resonator for a resonant micro-optic gyroscope," Opt. Lett. **42**(18), 3658 (2017).
9. J. Li, M.-G. Suh, and K. Vahala, "Microresonator brillouin gyroscope," Optica **4**(3), 346 (2017).
10. P. P. Khial, A. D. White, and A. Hajimiri, "Nanophotonic optical gyroscope with reciprocal sensitivity enhancement," Nat. Photonics **12**(11), 671–675 (2018).
11. J. Wiersig, "Review of exceptional point-based sensors," Photonics Res. **8**(9), 1457 (2020).
12. J. Wiersig, "Enhancing the sensitivity of frequency and energy splitting detection by using exceptional points: Application to microcavity sensors for single-particle detection," Phys. Rev. Lett. **112**(20), 203901 (2014).
13. M. Liertzer, L. Ge, A. Cerjan, A. D. Stone, H. E. Türeci, and S. Rotter, "Pump-induced exceptional points in lasers," Phys. Rev. Lett. **108**(17), 173901 (2012).
14. J. Ren, H. Hodaei, G. Harari, A. U. Hassan, W. Chow, M. Soltani, D. Christodoulides, and M. Khajavikhan, "Ultrasensitive micro-scale parity-time-symmetric ring laser gyroscope," Opt. Lett. **42**(8), 1556 (2017).
15. W. Chen, Ş. K. Özdemir, G. Zhao, J. Wiersig, and L. Yang, "Exceptional points enhance sensing in an optical microcavity," Nature **548**(7666), 192–196 (2017).
16. M. P. Hokmabadi, A. Schumer, D. N. Christodoulides, and M. Khajavikhan, "Non-hermitian ring laser gyroscopes with enhanced sagnac sensitivity," Nature **576**(7785), 70–74 (2019).
17. X. Mao, G.-Q. Qin, H. Yang, H. Zhang, M. Wang, and G.-L. Long, "Enhanced sensitivity of optical gyroscope in a mechanical parity-time-symmetric system based on exceptional point," New J. Phys. **22**(9), 093009 (2020).
18. G.-Q. Qin, R.-R. Xie, H. Zhang, Y.-Q. Hu, M. Wang, G.-Q. Li, H. Xu, F. Lei, D. Ruan, and G.-L. Long, "Experimental realization of sensitivity enhancement and suppression with exceptional surfaces," Laser Photonics Rev. **15**(5), 2000569 (2021).
19. D. Li, S. Huang, Y. Cheng, and Y. Li, "Compact asymmetric sound absorber at the exceptional point," Sci. China Phys. Mech. Astron. **64**(4), 244303 (2021).
20. X. Mao, H. Yang, D. Long, M. Wang, P.-Y. Wen, Y.-Q. Hu, B.-Y. Wang, G.-Q. Li, J.-C. Gao, and G.-L. Long, "Experimental demonstration of mode-matching and sagnac effect in a millimeter-scale wedged resonator gyroscope," Photonics Res. **10**(9), 2115 (2022).
21. D. Long, X. Mao, G.-Q. Qin, H. Zhang, M. Wang, G.-Q. Li, and G.-L. Long, "Dynamical encircling of the exceptional point in a largely detuned multimode optomechanical system," Phys. Rev. A **106**(5), 053515 (2022).
22. F. Nazari, M. Nazari, M. K. Moravvej-Farshi, and H. Ramezani, "Asymmetric evolution of interacting solitons in parity time symmetric cells," IEEE J. Quantum Electron. **49**(11), 932–938 (2013).
23. B. Peng, Ş. K. Özdemir, F. Lei, F. Monifi, M. Gianfreda, G. L. Long, S. Fan, F. Nori, C. M. Bender, and L. Yang, "Parity-time-symmetric whispering-gallery microcavities," Nat. Phys. **10**(5), 394–398 (2014).
24. X. Zhu, H. Ramezani, C. Shi, J. Zhu, and X. Zhang, "Pt symmetric acoustics," Phys. Rev. X **4**(3), 031042 (2014).
25. C. Yuce and H. Ramezani, "Robust exceptional points in disordered systems," EPL (Europhysics Lett.) **126**(1), 17002 (2019).
26. C. Yuce and H. Ramezani, "Diffraction-free beam propagation at the exceptional point of non-hermitian glauber fock lattices," Journal of Optics (2022).
27. B. M. Villegas-Martínez, F. Soto-Eguibar, S. A. Hojman, F. A. Asenjo, and H. M. Moya-Cessa, "Non-unitary transformation approach to pt dynamics," (2022).

Optical Materials EXPRESS

28. K. J. H. Peters and S. R. K. Rodriguez, "Exceptional precision of a nonlinear optical sensor at a square-root singularity," Phys. Rev. Lett. **129**(1), 013901 (2022).
29. C. Yuce and H. Ramezani, "Coexistence of extended and localized states in the one-dimensional non-hermitian anderson model," Phys. Rev. B **106**(2), 024202 (2022).
30. F. Yang, C. S. Prasad, W. Li, R. Lach, H. O. Everitt, and G. V. Naik, "Non-hermitian metasurface with non-trivial topology," Nanophotonics **11**(6), 1159–1165 (2022).
31. F. Lederer, G. I. Stegeman, D. N. Christodoulides, G. Assanto, M. Segev, and Y. Silberberg, "Discrete solitons in optics," Phys. Rep. **463**(1-3), 1–126 (2008).
32. H.-K. Lau and A. A. Clerk, "Fundamental limits and non-reciprocal approaches in non-hermitian quantum sensing," Nat. Commun. **9**(1), 4320 (2018).
33. N. A. Mortensen, P. Gonçalves, M. Khajavikhan, D. N. Christodoulides, C. Tserkezis, and C. Wolff, "Fluctuations and noise-limited sensing near the exceptional point of parity-time-symmetric resonator systems," Optica **5**(10), 1342–1346 (2018).
34. C. Wolff, C. Tserkezis, and N. A. Mortensen, "On the time evolution at a fluctuating exceptional point," Nanophotonics **8**(8), 1319–1326 (2019).
35. Z. Xiao, H. Li, T. Kottos, and A. Alù, "Enhanced sensing and nondegraded thermal noise performance based on p t-symmetric electronic circuits with a sixth-order exceptional point," Phys. Rev. Lett. **123**(21), 213901 (2019).
36. J. Wiersig, "Prospects and fundamental limits in exceptional point-based sensing," Nat. Commun. **11**(1), 2454 (2020).